Voltage Sources Exploration

Călina Burciu

February 2025

1 Abstract

The linear regression analysis in Task I confirmed a strong correlation between voltage and current, yielding an internal resistance of $R_i = 111.5 \pm 0.5\,\Omega$, a short-circuit current of $I_k = 27.64 \pm 0.13\,\text{mA}$, and a no-load voltage of $U_q = 3.0829 \pm 0.0033\,\text{V}$, with a coefficient of determination $r^2 = 0.9994$. In Task II, curve fitting resulted in $R_i = 110.44 \pm 1.49\,\Omega$ and $U_q = 3.0829 \pm 0.0033\,\text{V}$, demonstrating consistency within uncertainties. The experimental load resistance was found to be $R_a = 103.74 \pm 0.51\,\Omega$, slightly lower than the expected $R_a = 110.44 \pm 1.49\,\Omega$, indicating additional circuit resistances. The experimental power exceeded the expected value due to lower resistance, yielding $P_{\text{max, exp}} = 51.554 \pm 0.004\,\text{mW}$ at $R_a = 403.74 \pm 4.44\,\Omega$, $U_k = 4.590 \pm 0.026\,\text{V}$, and $I = 11.300 \pm 0.140\,\text{mA}$. Task III highlighted discrepancies in the I-V curve fitting, emphasizing the need for further analysis of the operating point region. Despite minor deviations, the results align with theoretical expectations, reinforcing the validity of the models used.

2 Introduction

This experiment explores the internal resistance and power characteristics of voltage sources by analyzing their voltage-current behavior. By varying the load resistance, key parameters such as internal resistance, no-load voltage, and short-circuit current are determined. Additionally, power dissipation is examined to identify conditions for maximum power transfer. A solar cell is also studied to determine its operating point and efficiency. Through data collection and analysis, this experiment provides practical insight into real-world deviations from ideal voltage sources.

3 Theoretical Basis

3.1 Characterization of a real voltage source

[1] A real voltage source consists of an ideal voltage source U_q (electromotive force, emf) and an internal resistance R_i. The terminal voltage U_k is given by:

$$U_k = U_q - IR_i \tag{1}$$

Where:

U_q = No-load voltage (V)
I = Current through the circuit (A)
R_i = Internal resistance of the source (Ω).

For a simple circuit with an ampermeter connected, the load resistance will be:

$$R_a = R_L + R_A \tag{2}$$

Where:

R_L = Resistance decade (Ω)
R_A = Internal resistance of the ampermeter (Ω).

By varying the load resistance R_a, the current I and voltage U_k can be measured. From Ohm's law:

$$I = \frac{U_q}{R_i + R_a} \tag{3}$$

This forms a linear relationship between U_k and I, allowing the determination of R_i from a linear fit of experimental data.

For the short-circuit condition $R_a \to 0$:

$$I_k = \frac{U_q}{R_i} \tag{4}$$

Where:

$$I_k = \text{Short-circuit current (A).}$$

The power dissipated by the load resistor R_a is given by:

$$P = I^2 R_a \tag{5}$$

Substituting I from Equation (2):

$$P = \left(\frac{U_q}{R_i + R_a}\right)^2 R_a \tag{6}$$

The maximum power transfer occurs when:

$$R_a = R_i \tag{7}$$

At this point, the maximum power is:

$$P_{\max} = \frac{U_q^2}{4R_i} \tag{8}$$

Where:

$$P = \text{Power dissipated (W).}$$

3.2 Characterization of a solar cell

[**?**]

A solar cell operates as a photovoltaic device that converts light energy into electrical energy. The performance of a solar cell is analyzed through its voltage-current (V-I) characteristics and power output.

A solar cell operates as a photodiode, and its current-voltage characteristic follows:

$$I_{solar} = I_S \left(e^{\frac{eV}{k_B T}} - 1\right) - I_{\text{Photo}} \tag{9}$$

Where:

$$\begin{aligned} I_S &= \text{Reverse bias current (A)} \\ V &= \text{Voltage across the solar cell (V)} \\ e &= 1.6021 \cdot 10{-}19 \text{ C} = \text{Elementary charge} \\ k_B &= 1.3806 \cdot 10^{-23} J/K = \text{Boltzmann's constant} \\ T &= \text{Temperature (K)} \\ I_{\text{Photo}} &= \text{Photo current (A).} \end{aligned}$$

At room temperature ($T \approx 300K$), the thermal voltage is given by:

$$\frac{k_B T}{e} \approx 25 \text{ mV} \tag{10}$$

For short-circuit current I_k and no-load voltage U_L:

$$I_k = -I_{\text{Photo}} \quad (\text{at } V = 0) \tag{11}$$

$$U_L = \frac{k_B T}{e} \ln\left(\frac{I_{\text{Photo}}}{I_S} + 1\right) \quad (\text{at } I = 0). \tag{12}$$

The power output of a solar cell is given by:

$$P = VI \tag{13}$$

To find the maximum power output, the P-R_a curve is analyzed. The operating point is the value of (V, I) where the power reaches its peak, known as the maximum power point (MPP). This occurs when:

By experimentally measuring voltage and current for different resistances R_a, we can determine the maximum power output and the corresponding resistance at which the solar cell operates most efficiently.

4 Experimental Setups

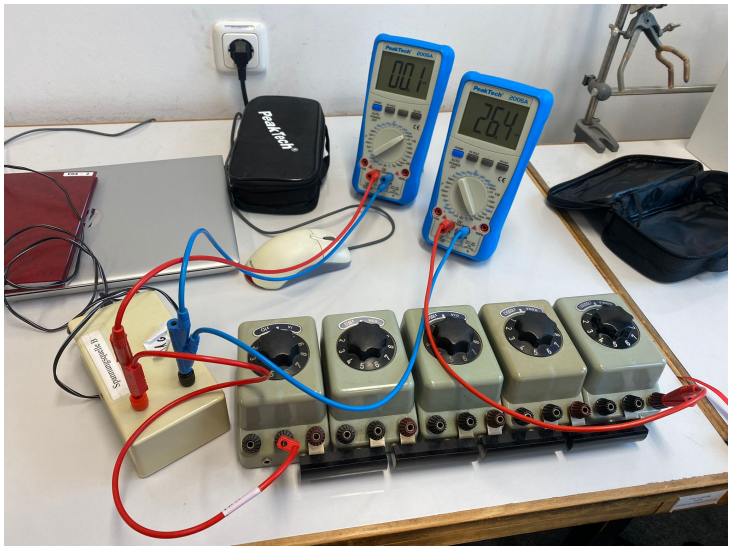

Figure 1: Simple Circuit with a Resistance Decade

The first experiment involves using a voltage source, two digital multimeter, a resistor decade box and connecting wires. The voltage source provides the required electromotive force, while the digital multimeter measures voltage and current. The resistor decade box allows precise variation of load resistance between 1Ω and $100k\Omega$.

For the voltage-current characteristic measurements, the voltage source is connected in series with a resistor decade box and a digital multimeter. A voltmeter is placed in parallel with the source to measure terminal voltage. The load resistance is varied systematically, and corresponding voltage and current values are recorded.

For power dissipation and maximum power transfer analysis, the same setup is used, ensuring that the multimeter resistance's internal, which measures the current, is accounted for. Power dissipation is calculated using the measured values, and a power-resistance curve is plotted to determine the condition for maximum power transfer.

In Task 3, a solar cell is used to determine photovoltaic performance, with an adjustable light source simulating sunlight.

For solar cell characterization, the solar cell is connected in series with a variable load resistor and the multimeter. A voltmeter is placed across the solar cell to measure terminal voltage. The solar cell is illuminated using a controlled light source. The load resistance is adjusted, and corresponding voltage and current readings are taken to construct the voltage-current characteristic. Power output is determined, and the maximum power point is identified by analyzing the power-resistance curve.

This setup ensures precise data collection and validation of theoretical predictions for voltage sources and photovoltaic performance.

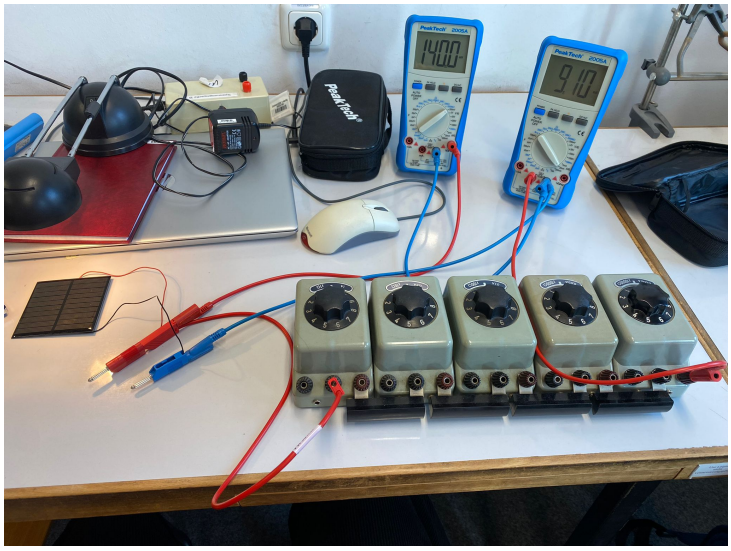

Figure 2: Solar Cell Circuit

5 Data Analysis

For Task I, the linear regression in Fig. 3 was performed over R_i, I_k, and U_q using Eq. 1. The graph demonstrates a linear relationship between the voltage and the current, enabling a linear fit. From this fit, the internal resistance is determined as $R_i = 111.5 \pm 0.5\Omega$, the short-circuit current is $I_k = 27.64 \pm 0.13mA$ and no-load voltage is $U_q = 3.0829 \pm 0.0033V$, with a $r^2 = 0.9994$. This value of r^2 indicates a strong correlation between the model and the actual data, reinforcing confidence in the parameters obtained through the curve fitting process.

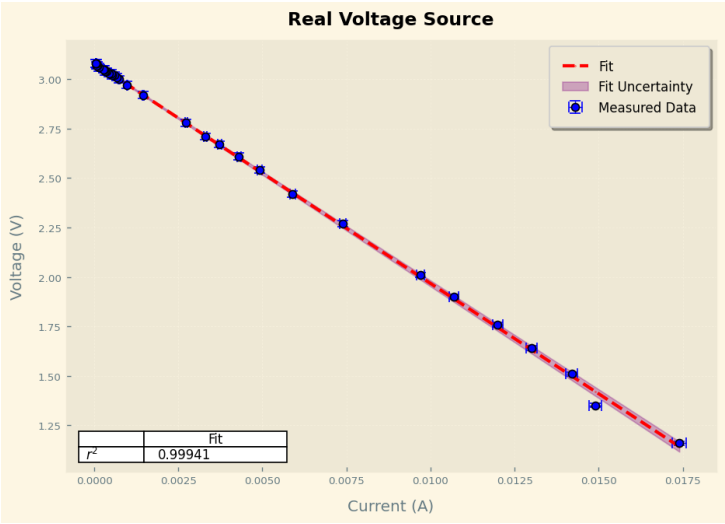

Figure 3: Task I - Linear Regression

In Task II, the Fig. 4 is a P-R_a diagram is required to identify the maximum power and its corresponding load resistance R_a. The expected value was calculated using Eq. 8, yielding $P_{\text{expected}} = 21.32 \pm 0.38mW$ at $R_a = R_i = 110.44 \pm 1.49\Omega$ using the internal resistance determined through the curve fitting process, with an $r^2 = 0.9996$. The maximum experimental power value was obtained by identifying the peak power from the measured data as $P_{experimental} = 21.44 \pm 1.83mW$ at $R_a = 103.74 \pm 0.51\Omega$. This ensures consistency between the theoretical predictions and the experimentally obtained values, validating the applied model. Other values found in the curve fit of the measured data were the resistance of the amperemeter $R_A = 3.7 \pm 2.4\Omega$ and the no-load voltage $U_q = 3.069 \pm 0.018V$.

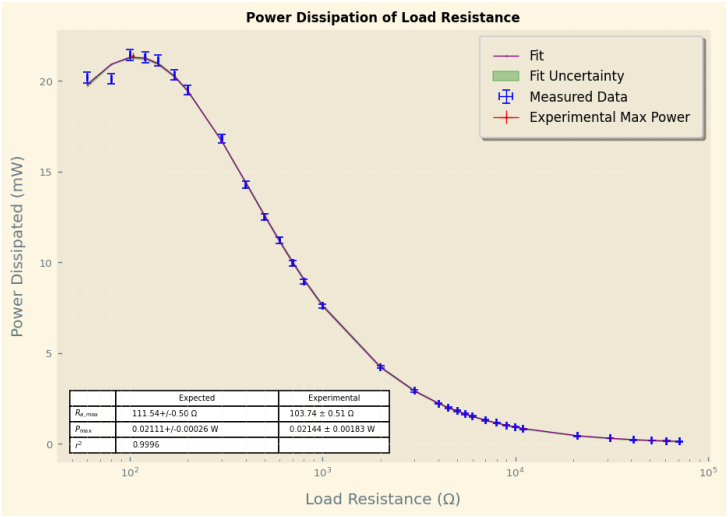

Figure 4: Task II - Power Dissipation of R_a

In Task III, a solar cell is analysed, trying to fin the operating point and the power generated at this point. In Fig. 5, the experimental value of the power at the operating point was $P = 51.554 \pm 0.004mW$ at $R_a = 403.74 \pm 4.44\Omega$, with a corresponding terminal voltage $U_k = 4.590 \pm 0.026V$ and current $I = 11.300 \pm 0.140mA$.

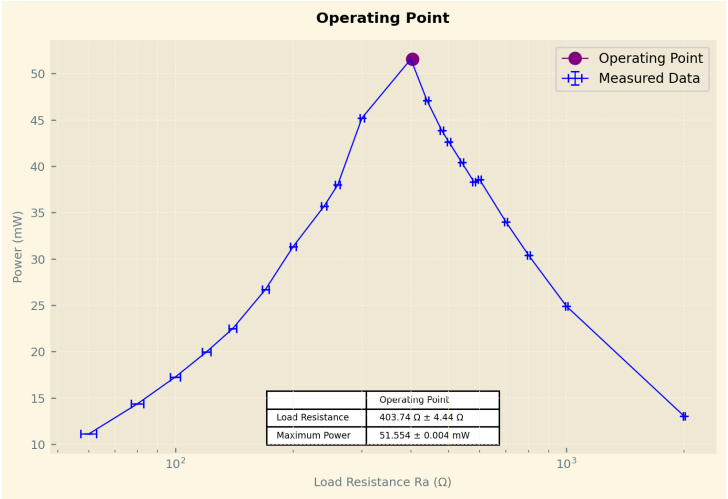

Figure 5: Task III - Operating Point

As an additional perspective on the solar cell circuit, the graph in Fig. 6 was analyzed. Overall, the curve fit on the I-V characteristic was not as successful, as the operating point does not lie on the curve formed by the no-load voltage and the short-circuit current. This deviation suggests potential inaccuracies in the curve fit, making it appear unreliable. The discrepancy could be attributed to external influences such as contact resistance, temperature variations, or non-ideal diode effects, impacting the accuracy of the model approximation.

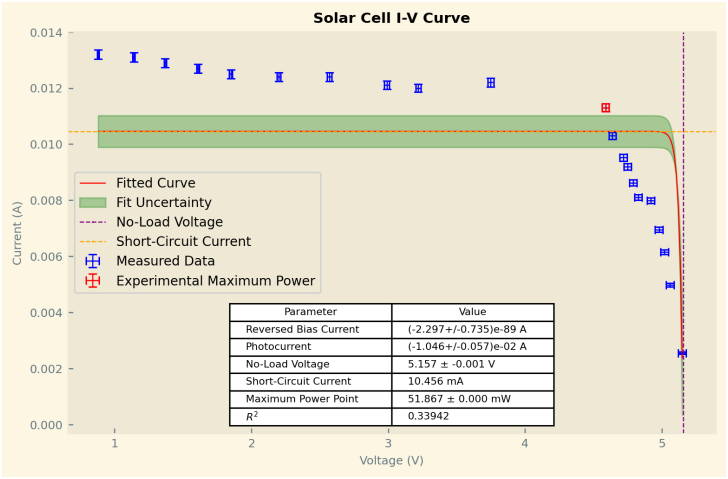

Figure 6: Task III - Solar I-V Curve

6 Discussion

The linear regression analysis in Task I, applied to R_i, I_k, and U_q using Eq. 1, confirms a strong linear relationship between voltage and current, validating the use of a linear fit. The extracted parameters from the fit indicate an internal resistance of $R_i = 111.5 \pm 0.5\Omega$, the short-circuit current is $I_k = 27.64 \pm 0.13mA$, and the no-load voltage is $U_q = 3.0829 \pm 0.0033V$, with a $r^2 = 0.9994$.

The high coefficient of determination, $r^2 = 0.9994$, signifies an excellent agreement between the experimental data and the model, ensuring confidence in the accuracy of the estimated parameters. The minimal uncertainties suggest high measurement precision, although minor discrepancies could still arise from external influences such as contact resistance, instrumental limitations, or environmental fluctuations. These variations could slightly affect the measured values, but the overall consistency of the data supports the validity of the findings.

The data can be considered reliable and trustworthy, as the process was straightforward without significant complications. The agreement between the theoretical expectations and the fitted parameters further reinforces the results.

For the curve fit in Task II, although different values were obtained for the same physical parameters as in Task I using essentially the same experimental data, they remain within the range of their uncertainties. Generally, as curve fitting has a higher rate of failure compared to linear regression, the stronger correlation with the measured data, represented by the coefficient of determination r^2, ensures greater accuracy in the estimated parameters. Since the internal resistance is determined as $R_i = 110.44 \pm 1.49\Omega$ and the no-load voltage as $U_q = 3.0829 \pm 0.0033V$, these values remain valid as the observed differences arise from the distinct computational approaches—linear regression and curve fitting—used in the analysis.

Additionally, the resistance of the amperemeter, $R_A = 3.7 \pm 2.4\Omega$, is not the only resistance present in the circuit. The experimental value of $R_a = 103.74 \pm 0.51\Omega$ is found to be smaller than the expected $R_a = 110.44 \pm 1.49\Omega$, indicating the presence of additional small resistances in the circuit, such as those from cables, connections, and minor contact resistances. These unaccounted resistances, although small, contribute to slight deviations in the expected values. A lower actual resistance results in a higher actual power output, as observed in the graph, explaining why the experimental power exceeds the expected value. This discrepancy is common in practical circuits, where idealized theoretical assumptions do not fully account for all contributing factors.

In Task III, the focus should be on the $P-R_a$ diagram as the curve fit of the I-V curve did not succeed. The operating point was found by measuring the maximum value of the power $P_{max} = 51.554 \pm 0.004mW$ and its corresponding resistance $R_a = 403.74 \pm 4.44\Omega$, terminal voltage $U_k = 4.590 \pm 0.026V$, and current $I = 11.300 \pm 0.140mA$. These values were identified by systematically varying the load resistance and observing the peak power generation point. The deviation of the experimental maximum power point from the theoretically predicted value suggests that additional factors, such as dynamic resistive elements, minor internal losses, or environmental conditions, may have played a role in the measurements.

Although I state that the I-V curve is not perfectly constructed, it highlights important aspects of the circuit. The discrepancies observed in the curve fitting process suggest that the model could be improved

by considering more complex representations of the solar cell behaviors. Despite this, the analysis still provides some insights into the characteristics of the system. In the case of a battery or a solar cell, the current naturally flows in a direction that results in a negative value, indicating that the device is supplying energy. Consequently, the power, given by $I \cdot V$, is also negative, reinforcing the fact that the system is acting as a generator rather than a load, resulting in the name of "Operating point". This behavior aligns with the expected performance of power sources, where energy is delivered to an external circuit.

The combined findings across all tasks demonstrate the effectiveness of both theoretical models and experimental validation in analyzing electrical circuits. The observed differences between expected and experimental values highlight the importance of considering real-world factors, ensuring a comprehensive understanding of the system's performance. For further analysis, it is recommended to take a closer look at the region where the operating points can be located, rather than focusing on higher resistance values where the saturation voltage becomes dominant.

References

[1] Walker Halliday, Resnick. *Fundamentals of Physics*, chapter 27, pages 710–714. Wiley, eighth edition.